
This copy is for your personal, non-commercial use only.

If you wish to distribute this article to others, you can order high-quality copies for your colleagues, clients, or customers by [clicking here](#).

Permission to republish or repurpose articles or portions of articles can be obtained by following the guidelines [here](#).

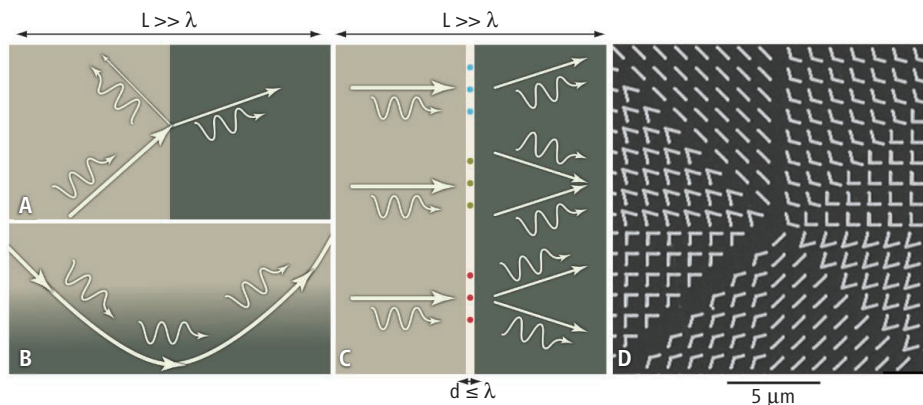
The following resources related to this article are available online at www.sciencemag.org (this information is current as of October 21, 2011):

Updated information and services, including high-resolution figures, can be found in the online version of this article at:

<http://www.sciencemag.org/content/334/6054/318.full.html>

This article **cites 15 articles**, 3 of which can be accessed free:

<http://www.sciencemag.org/content/334/6054/318.full.html#ref-list-1>



Bending light, big and small. Several mechanisms for bending light are depicted. The optical structures shown in (A) and (B) are much larger than the wavelength of light. In (A), an interface between two media with two different indices of refraction bends light. In (B), light is bent by a material that gradually changes refractive index with distance. Yu *et al.* caused the bending of light in unusual ways (C) with thin metasurfaces. These metasurfaces contain distributed arrays of gold nanoantennas (D) that are smaller than the wavelength of light. In such arrays, the proper patterns of phase changes created by resonant nanostructures lead to bending effects not anticipated by conventional laws of reflection and refraction in optics.

gold antennas with a V shape; they varied the scattering of light by changing the length of the arm and the angle and the orientation of these “V’s.” The phase difference between the scattered and incident fields is tailored over a small distance along the light’s path, that is, the structures are optically thin.

Yu *et al.* printed planar arrays of such V-shaped nanoantennas in suitably designed patterns on a silicon wafer and demonstrated several intriguing light-bending scenarios at these metasurfaces, including unconventional reflection and refraction angles, total internal reflections with two critical angles (rather than only one), and reflected light becoming evanescent (diminishing in amplitude with distance away from the interface, rather than propagating) at certain angles. None of these effects are predicted from the conventional Snell’s law, but they do follow a generalized version derived by the authors that allows for desired variations of the change of phase on the interface.

These arrays of nanoantennas, which could include movable sections, could be used to design photonic components such as lenses and mirrors that are ultrathin, conformal (angle-preserving), and even deformable. Reconfigurable couplers and waveguides, which could be driven by electric, magnetic, or optical stimuli, may be envisioned that could guide and mix light beams through almost arbitrary paths chosen along a surface. Yu *et al.* have also created optical vortices with orbital angular momentum (6) by impinging a beam at normal incidence on the specially designed planar metasurface of these V-shaped nanoantennas. Such vortices could find use in applications such as optical tweezers.

Metasurfaces (7) are the planar version of metamaterials that are engineered to control and tailor the light interaction in unconventional ways (for example, creating materials with optical band gaps that completely reflect light over a given frequency range). In the three-dimensional metamaterials, it can be difficult to engineer a structure that maintains its designed performance and avoids performing like a bulk material. Meta-

surfaces may offer advantages in this regard because their constituent resonant elements are all distributed in a planar surface and more readily assembled. This type of two-dimensional structure will add another tool to the field of transformation optics (8, 9), in which a prescribed change (such as a phase shift or amplitude variation) is designed into the light path for applications such as cloaking, or where metasurfaces are used to creating highly confined cavity modes (10, 11) of potential interest in quantum optics.

References

1. M. Born, E. Wolf, *Principles of Optics* (Pergamon, Oxford, 1980).
2. N. Yu *et al.*, *Science* **334**, 333 (2011).
3. D. M. Pozar, S. D. Targonski, H. D. Syrigos, *IEEE Trans. Antenn. Propag.* **45**, 287 (1997).
4. C. G. M. Ryan *et al.*, *IEEE Trans. Antenn. Propag.* **58**, 1486 (2010).
5. N. Bliznyuk, N. Engheta, *Mic. Opt. Tech. Lett.* **40**, 361 (2004).
6. M. Padgett, J. Courtial, L. Allen, *Phys. Today* **57**, 35 (2004).
7. E. F. Kuester, M. A. Mohamed, M. Piket-May, C. L. Holloway, *IEEE Trans. Antenn. Propag.* **51**, 2641 (2003).
8. J. B. Pendry, D. Schurig, D. R. Smith, *Science* **312**, 1780 (2006).
9. U. Leonhardt, *Science* **312**, 1777 (2006).
10. M. Caiazzo, S. Maci, N. Engheta, *IEEE Antenn. Wirel. Propag. Lett.* **3**, 261 (2004).
11. C. L. Holloway, D. C. Love, E. F. Kuester, A. Salandrino, N. Engheta, *IET Microwave Antenn. Propag.* **2**, 120 (2008).

10.1126/science.1213278

OCEANS

Eddies Masquerade as Planetary Waves

Dennis J. McGillicuddy Jr.

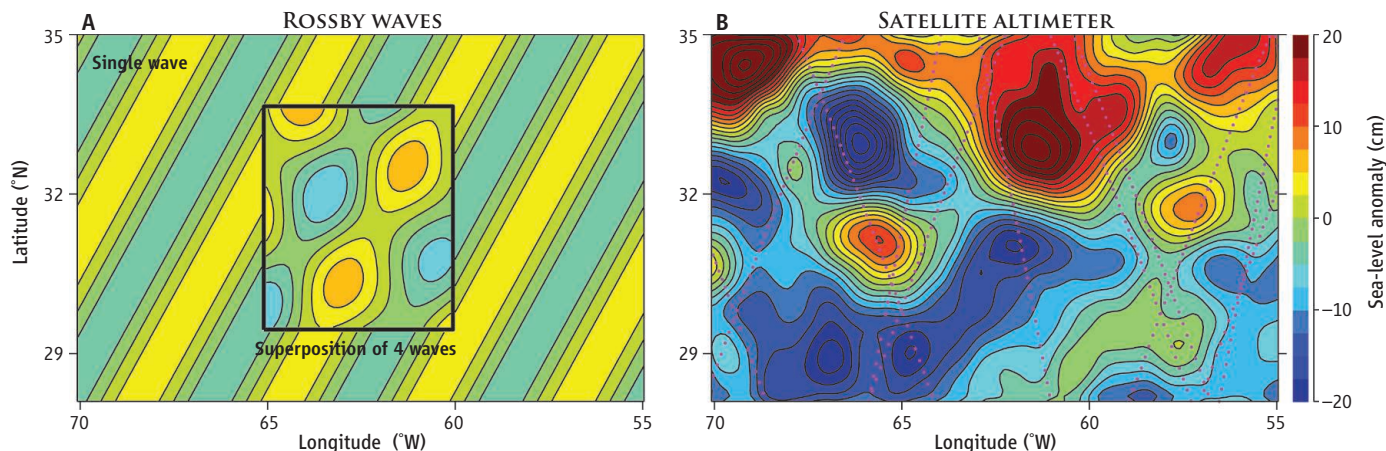
Variabilities in sea-level and upper-ocean chlorophyll reveal the systematic influence of nonlinear eddies.

The advent of satellite-based remote sensing of ocean color in the late 1970s (1) provided the first large-scale views of chlorophyll distributions in the upper ocean. These distributions are a proxy for the biomass of phytoplankton, which drive oceanic productivity. More recently, ocean color measurements have been combined with satellite data on sea-surface height (SSH) and other physical properties of the ocean to elucidate the processes that regulate primary production in

the sea. On page 328 of this issue, Chelton *et al.* (2) further advance this field by showing that ocean eddies exert a strong influence on near-surface chlorophyll.

Initial comparisons (3, 4) of satellite ocean color measurements and SSH data showed that some of the variability in ocean color was associated with large-scale SSH patterns that propagate westward in extratropical latitudes. The authors attributed these patterns to planetary or Rossby waves, which are freely propagating modes of large-scale variability in the ocean. Four basic processes have been proposed to explain the observed relations, including lateral

Woods Hole Oceanographic Institution, Woods Hole, MA 02543–1541, USA. E-mail: dmcgillicuddy@whoi.edu



Rosby waves and eddies. (A) A model of a single Rossby wave propagating through a still ocean leads to a highly regular sea-level anomaly pattern. If several such waves are superposed, an eddy-like pattern results (inset) (15). (B) Mapped observations (16) of sea-level anomaly for a region of the western North

Atlantic on 17 June 2005. Satellite ground tracks are shown as dotted lines. Although the patterns seen in the altimeter data resemble those of the superposed Rossby waves, Chelton *et al.* show that they are in fact caused by nonlinear mesoscale eddies.

advection of the mean chlorophyll gradient, uplift of the deep chlorophyll maximum into the surface layer, enhancement of phytoplankton biomass stimulated by upwelling of nutrients, and accumulation of material in convergence zones within the planetary wave field (5–7).

These early studies focused on large-scale signals characteristic of Rossby waves by processing the satellite measurements with scale-selective filters. This processing was intended to remove seasonal variability as well as the effects of mesoscale (tens to hundreds of kilometers) eddies—ubiquitous features of ocean circulation (sometimes referred to as the internal weather of the sea) that result from both direct forcing and internal instability processes.

Merging data from multiple satellite missions led to altimetric data sets (8–10) with higher resolution than used previously, but it remains difficult to differentiate between Rossby waves and eddies in the merged data sets. Single Rossby waves (see the figure, panel A) are rarely if ever observed in the ocean, but superposition of multiple Rossby waves can result in eddy-like features (panel A, inset) that are similar to the patterns seen in altimeter data (panel B). However, planetary waves and eddies have different degrees of nonlinearity: Nonlinear eddies trap fluid inside them, whereas linearly propagating wavelike disturbances do not. The degree of nonlinearity can be estimated as the ratio between an eddy's swirl velocity and its translation speed.

Previously, Chelton and co-workers used this insight to show that mid-latitude SSH variability is dominated by westward-propagating nonlinear eddies, and developed automated tracking algorithms to compile a

global synthesis of eddy trajectories (9, 10). Chelton *et al.* have now overlaid those eddy tracks on the westward-propagating signals previously attributed to Rossby waves in the filtered SSH and ocean color data. The results strongly suggest that eddies are driving these signals (2).

How might mesoscale eddies masquerade as larger-scale Rossby waves? Due to the latitudinal dependence of the effects of Earth's rotation, both types of features move westward at roughly the same speed. Moreover, Chelton *et al.* show that the statistical properties of a patchwork of westward-propagating eddies are qualitatively similar to those expected for Rossby waves. This observation explains why eddies can pass through the filters intended to eliminate them in earlier studies.

Chelton *et al.*'s findings require reassessment of the underlying mechanisms used to explain satellite observations of variability in SSH and upper-ocean chlorophyll. Although the same four basic processes of biomass modulation mentioned above for Rossby waves remain valid for eddies, lateral advection of the mean chlorophyll gradient is the dominant mechanism revealed in Chelton *et al.*'s analysis. However, the relative importance of each of the four processes can vary with oceanographic regime and scale, ranging from the mesoscale down to the submesoscale (11–13). At present, submesoscale features are not resolved by operational remote-sensing technology for SSH.

Although higher-resolution data are expected in the future for both SSH and ocean color, in situ observations will continue to be critical for those variables that cannot be measured from space. Moreover, because near-surface waters are depleted in

nutrients over large areas of the mid-latitudes, key aspects of the biological response to physical perturbations take place too deep to be detected by satellite ocean color imagery (14). Although Chelton *et al.*'s results must be interpreted with that caveat, their findings constitute a key step forward in our understanding of physical-biological interactions in the ocean, with important ramifications for both ecosystem dynamics and biogeochemical cycling.

References and Notes

1. J. F. R. Gower, K. L. Denman, R. J. Holyer, *Nature* **288**, 157 (1980).
2. D. B. Chelton, P. Gaube, M. G. Schlax, J. J. Early, R. M. Samelson, *Science* **334**, 328 (2011); 10.1126/science.1208897.
3. B. M. Uz, J. A. Yoder, V. Osychyn, *Nature* **409**, 597 (2001).
4. P. Cipollini, D. Cromwell, P. G. Challenor, S. Raffaglio, *Geophys. Res. Lett.* **28**, 323 (2001).
5. P. D. Killworth, P. Cipollini, B. M. Uz, J. R. Blundell, *J. Geophys. Res.* **109**, C07002 (2004).
6. Y. Dandonneau, A. Vega, H. Loisel, Y. du Penhoat, C. Menkes, *Science* **302**, 1548 (2003).
7. G. Charria, F. Mélin, I. Dadou, M.-H. Radenac, V. Garçon, *Geophys. Res. Lett.* **30**, 1125 (2003).
8. A. Pascual, Y. Faugère, G. Larnicol, P.-Y. Le Traon, *Geophys. Res. Lett.* **33**, L02611 (2006).
9. D. B. Chelton, M. G. Schlax, R. M. Samelson, *Prog. Oceanogr.* **91**, 167 (2011).
10. D. B. Chelton, M. G. Schlax, R. M. Samelson, R. A. de Szoeke, *Geophys. Res. Lett.* **34**, L15606 (2007).
11. M. Lévy, P. Klein, A.-M. Treguier, *J. Mar. Res.* **59**, 535 (2001).
12. E. R. Abraham, *Nature* **391**, 577 (1998).
13. D. A. Siegel, P. Peterson, D. J. McGillicuddy Jr., S. Mariotorena, N. B. Nelson, *Geophys. Res. Lett.* **38**, L13608 (2011).
14. D. J. McGillicuddy Jr. *et al.*, *Science* **316**, 1021 (2007).
15. J. C. McWilliams, G. R. Flierl, *Deep-Sea Res.* **23**, 285 (1976).
16. Altimeter data were produced and distributed by AVISO (www.aviso.oceanobs.com) as part of the SSALTO ground-processing segment.
17. I thank NSF and NASA for support and L. Anderson for preparing the figure.

10.1126/science.1208892